DRAFT VERSION NOVEMBER 3, 2014
Preprint typeset using LaTeX style emulateapj v. 12/16/11

PROBING THE INNER KPC OF MASSIVE GALAXIES WITH STRONG GRAVITATIONAL LENSING

YASHAR D. HEZAVEH, PHILIP J. MARSHALL, ROGER D. BLANDFORD
Kavli Institute for Particle Astrophysics and Cosmology, Stanford University, Stanford, CA, USA
Draft version November 3, 2014

ABSTRACT

We examine the prospects of detecting demagnified images of gravitational lenses in observations of strongly lensed mm-wave molecular emission lines with ALMA. We model the lensing galaxies as a superposition of a dark matter component, a stellar component, and a central supermassive black hole and forecast the detection of the central images for a range of relevant parameters (e.g. stellar core and black hole mass). We find that over a large range of acceptable parameters, future deep observations of lensed molecular lines with ALMA should be able to detect the central images at $\gtrsim 3\sigma$ significance. We use a Fisher analysis to examine the constraints that could be placed on these parameters in various scenarios and find that for large stellar cores, both the core size and the mass of the central SMBHs could be measured. We also study the prospects of detecting binary SMBHs in such observations, and find that only under very rare condition such observations could be

Subject headings: black hole physics — gravitational lensing: strong — galaxies: formation — galaxies: high-redshift

1. INTRODUCTION

Probing the matter distribution in the innermost kpc of galaxies can answer key questions about super massive black holes (SMBH), galaxy formation, and dark matter. It is now established that almost every massive galaxy harbors a SMBH at its center with a mass that strongly correlates with the mass of the host galaxy (Kormendy & Richstone 1995; Ferrarese & Merritt 2000; Gebhardt et al. 2000; Tremaine et al. 2002). In addition, the distribution of stellar populations in central regions of galaxies contains information about their past merger histories and SMBH-stellar population interactions. (e.g Barnes & Hernquist 1992; Ebisuzaki et al. 1991). Various dark matter models also predict different structures for the central regions of dark matter halos (e.g Rocha et al. 2013). Mapping the matter density in the central regions of galaxies can thus shed light on various astrophysical phenomena.

Studies of local galaxies in optical wavelengths have shown that, unlike their lower-mass counterparts, the most massive elliptical galaxies often exhibit cored stellar light profiles, with core sizes ranging from 50 to 500 pc (e.g., Ferrarese et al. 2006). These galaxies are thought to form through gas-poor mergers. In such mergers, the central structure of the resulting galaxy is dominated by the inner structure of the more concentrated progenitor. Since high-mass ellipticals are thought to form from mergers of their lower-mass counterparts, with steep profiles, the existence of cores in these galaxies represents a challenge to our understanding of galaxy mergers. Cores in massive ellipticals, therefore, should be the result of different (not merger) mechanisms. "Black hole scouring" is a plausible mechanism that can explain core-formation in these galaxies (Thomas et al. 2014).

It is thought that during a merger, the SMBHs of the two merging galaxies form a binary which sinks to the center of the potential. The two orbiting SMBHs then dissipate angular momentum through three-body interactions with nearby central stars, pushing the stars to higher orbits and "scouring out" a core. This angular momentum loss then allows the two black holes to merge (Begelman et al. 1980). Previous studies have shown that the core sizes in these galaxies scale with the mass of their SMBHs, in agreement with theoretical predictions (Kormendy & Bender 2009; Kormendy & Ho 2013). Such measurements, however have been limited to low redshifts, since both dynamical measurements to constrain the stellar and SMBH masses, and morphological measurements to constrain core sizes require very high physical resolutions.

Strong gravitational lensing is a powerful tool for probing the matter distribution in distant galaxies. Among other things, strong lenses have been used to constrain galaxy masses (e.g.), density profiles (e.g.), and abundance of dark matter subhalos (e.g.). The strong lensing theory indicates that the number of lensed images should always be odd. For double and quad image configurations, a third and a fifth image are predicted to exist near the centers of lensing galaxies. Unlike the other lensed images, which are magnified, this image can be significantly *demagnified*, making its detection difficult (). It is well-understood that the magnification of the central images is very sensitive to the matter distribution in the innermost regions of lens galaxies: very steep singular density profiles significantly demagnify the central images, whereas cored or shallow profiles render them brighter. In addition to their low flux, the fact that central images coincide with the emission from lens galaxies makes their detection even harder. Distinguishing the central images from emission originating in the lens galaxies is extremely challenging. Moreover, if observed in the optical, absorption in the central dense regions of the lens can make the central images even dimmer, while the photon noise from the lens emission further reduces the sensitivity.

The individual behavior and statistical properties of central images in lensed populations have been extensively studied (e.g. Wallington & Narayan 1993; Evans & Hunter 2002; Keeton 2003). These studies show that central images could have a wide range of magnifications (e.g., Keeton 2003). Observational searches for these images have found a number of candidates (e.g.). Although observations of central images in group and cluster lenses are not uncommon (e.g., Inada et al. 2005), only one secure detections of a central image of a galaxy-scale lens exists to date (Winn et al. 2004). To avoid the possibility of absorption in the lens, most searches have focused on strongly lensed radio quasars and the radio spectrum of candidate central images have been used to distinguish them from potential faint emission from the lens galaxies.

A new large population of strong lenses has recently been discovered in mm-bands. These systems were initially detected as bright point sources in wide area mm/submm surveys (Vieira et al. 2010; Negrello et al. 2010). Follow-up observations have confirmed that they constitute a large population of strong lenses (Vieira et al. 2013; Hezaveh et al. 2013; Bussmann et al.

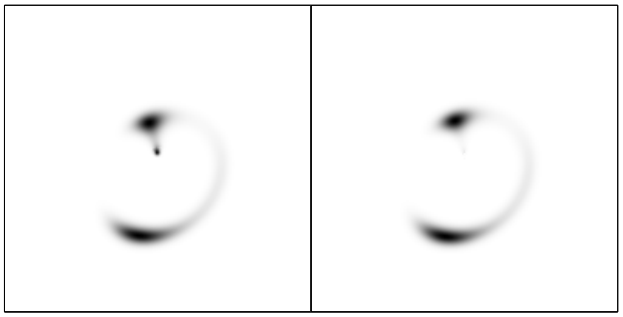

FIG. 1.— illustration of the central image in 2 cases:

2013). In particular, ALMA observations of these sources have revealed that the background galaxies are dusty, starburst, high redshift galaxies, containing a wealth of cold molecular gas (Weiß et al. 2013). These observations showed that the extreme brightness of the sources in combination with the high sensitivity of ALMA results in very high signal to noise ratios (e.g. the lens models in Hezaveh et al. 2013, were based on just ~ 50 second long observations). Motivated by the discovery of this population and the operation of ALMA, here we revisit the issue of detecting central images. Deep ALMA observations of molecular line emission in these sources are likely to be carried out for various reasons (e.g., Hezaveh et al. 2014; Hezaveh 2014). If a central image of a lensed molecular line is detected, it will be readily identifiable since it will correspond to the redshift of the source, leaving no doubt about its origin. In addition, since these lines are in mm-bands, the line fluxes are very unlikely to be suppressed due to absorption in the lens. In contrast to lensed quasars, these sources are extended over hundreds of parsecs and can cover a larger area of the source plane. This can allow them to occupy the less demagnified regions of the source plane, allowing a higher flux for the central image (the opposite effect of magnification damping due to extended sources, see e.g., Hezaveh & Holder 2011).

In this letter, we explore the possibility of detecting central lensed images in such deep observations and investigate the constraints that could be placed on the core size, mass of SMBHs, and the slope of the density profiles from detection, or non-detection of such images. We also examine if binary SMBHs can possibly be detected in such observations. In Section 2 we describe the simulations, in Section 3 we present the results and discuss them, and finally conclude in Section 4. We use a flat ΛCDM cosmology with $h = 0.71$ and $\Omega_M = 0.267$.

2. SIMULATIONS

We generated lensed images of background sources, predicted ALMA visibilities, and used them to estimate the detection significance of central images for various parameters. We simulated observations of a high-J CO line. The line is assumed to have a velocity integrated flux of 1 Jy km/s and a FWHM of 400 km/s, resulting in an average flux of 2.5 mJy over a 400 km/s band.

We modeled the lens potential as a sum of three components: dark matter, stellar population and central SMBH. The dark matter was modeled as a singular power-law with a slope of 0.1, in agreement with the projected surface mass density of the NFW profile (Golse & Kneib 2002). As by pointed out by (Keeton 2003), due to its extreme flatness in these regimes, the dark matter component has negligible influence on the central images. The stellar population is modeled as a a core power-law, $\Sigma \propto (r^2 + R_{\rm core}^2)^{\gamma}$. Figure 2 shows the stellar component (red curve), dark matter component (black dashed curve) and the sum of the two (black solid curved). The grey dashed curves show a few example of core-sersic models with

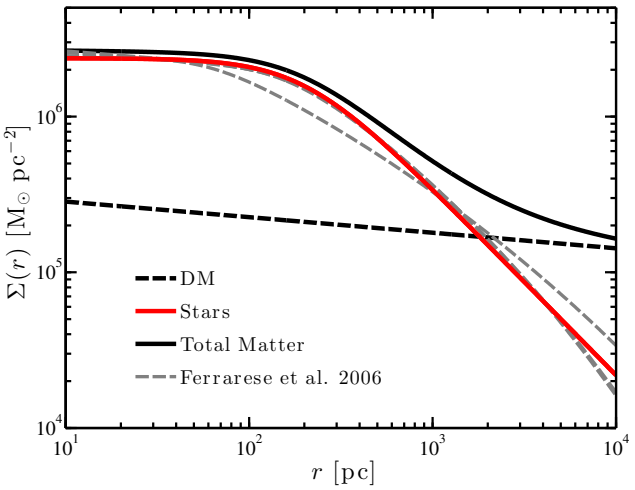

FIG. 2.— Model density profiles. The black dashed line shows the dark matter component, with a slope of 0.1, consistent with a projected NFW at the innermost regions. the grey dashed curves show cored-sersic five fits to stellar light profiles of massive galaxies from Ferrarese 2006. The red solid curve shows our cored-power-law model that we use to approximate this stellar component. The solid black line shows the total matter density (dark plus stellar) of our model.

parameters taken from Ferrarese et al. (2006). Although the cored power-law model used in this work does not account for the slope of the stellar distribution below the core break, it is a close fit and a reasonable model to approximate the observed stellar light profiles. The black hole was modeled as a simple point mass at the center of the potential. We assumed that all the three components are concentric. The stellar and dark mass of the lens were normalized such that they each add up to $1.5 \times 10^1 1 M_\odot$ in a radius of 10 kpc. The resulting Einstein radius if of order 1 arcsec, in agreement with galaxy-galaxy strong lenses (e.g.,). To predict the visibilities we calculated the ALMA uv-coverage for a 5-hr long observation (full array), using the $simobserve$ task of Common Astronomy Software Applications package, for an observing frequency of 150 GHz. The visibilities for each channel were calculated by computing the 2D Fourier transform of the surface brightness data maps and resampling the Fourier transform maps over the uv-coverage. The noise was estimated using ALMA sensitivity calculator for a channel width of 400 km/s at 150 GHz.

For simulations where we calculated the detection significance of the demagnified image, we computed the magnification at every pixel in the image plane and generated maps with and without the the demagnified flux and evaluated the detection significance of the central image by comparing the two images. In other simulations where the constrains on parameters are needed, we used a Fisher analysis to compute the full covariance of all parameters. We used finite differencing of visibilities to calculate the gradients, and marginalize over the nuisance parameters (e.g. source position, lens ellipticity) to calculate the marginalized likelihood of the relevant parameters.

3. RESULTS AND DISCUSSIONS

3.1. *Detection of central images with ALMA*

As discussed earlier, the fluxes of central images strongly depend on the slope of the lensing potential, the core size, and the mass of the central SMBHs. Figure 3 shows the detection significance of a central image for a range of these parameters in a 10-h long ALMA observation. The grey curves (dark to light) correspond to profiles with slopes of $\gamma = 0.9, 1.0, 1.1,$ and 1.2. As seen in this figure, larger stellar cores result in brighter images. When $\gamma = 1.0$ and with a core size larger than 150 pc, such observations should be able to detect the central

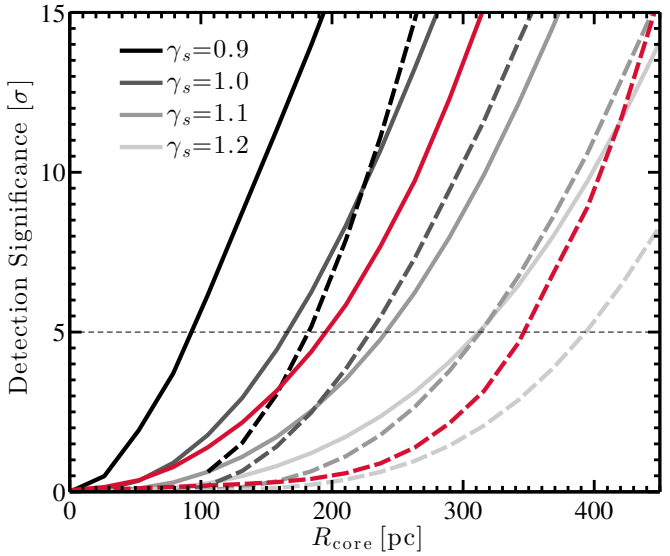

FIG. 3.— Detection significance of a central image as a function of the stellar core size for a 10-hr long ALMA observation. The gray shades correspond to different slopes for the stellar component. The solid curves correspond to a case without a SMBH while the dashed curves show the results when a $2 \times 10^8 M_\odot$ SMBH is placed at the center of the lens. The source has a Gaussian light profile with an rms of 600 pc. The red curves show the same predictions when $\gamma = 1$, for a source with rms of 300 pc.

images with more than 5σ significance. For significantly shallower ($\gamma < 0.8$) profile slopes with larger cores, the central image is *magnified* and its detection should be trivial. The magnification and flux of central images is also influenced by SMBHs. SMBHs demagnify the images on scales comparable to the size of their Einstein radii ($\sim$ 30 mas for a $2 \times 10^8 M_\odot$ SMBH). The dashed curves in Figure 3 show the suppression of the fluxes of central images in presence of a $2 \times 10^8 M_\odot$ SMBH.

As seen in Figure 3, and as pointed out by Keeton (2003), plausible parameters (e.g. core sizes) predict a wide range of magnifications for central images. Although for some plausible parameter combinations (e.g., $\gamma_s = 1.2$, $M_{BH} = 2 \times 10^8 M_\odot$,$R_{core} < 300pc$) there is little chance of detecting the central images, over a non-negligable fraction of parameter space the central images may be detectable.

We also find that the detection significance of the central images can increase by about 3σ for an extended source with a radius of 1 kpc compared to a point source. Since extended sources occupy a larger area of the source plane, which may cover regions with higher magnifications, the resulting flux can be larger than the flux of more compact sources.

3.2. *SMBHs and the core size*

We studied the constraints that could be placed on the slope of the density profile, the size of the stellar core, and the mass of the SMBHs in such deep observations. We performed a Fisher analysis to examine the constrains and parameter degeneracies in simulations in which the central images are detected, as well as those in which they are below the detection limit. All model parameters were included in the Fisher matrix, and nuisance parameters were later marginalize over (e.g. intrinsic source flux and position) to obtain the marginalized likelihood of the relevant parameters. Figure 4 shows the parameter covariance for two examples with different core radii (top panel: R_{core}=170 pc, bottom panel: R_{core}=450 pc). We found that when $\gamma = 1$, core sizes larger than 100 pc can be measured with high significance. As seen in top panel of Figure 4, the mass of SMBH is degenerate with the core size: larger cores result in brighter images, whose flux can be supressed by a

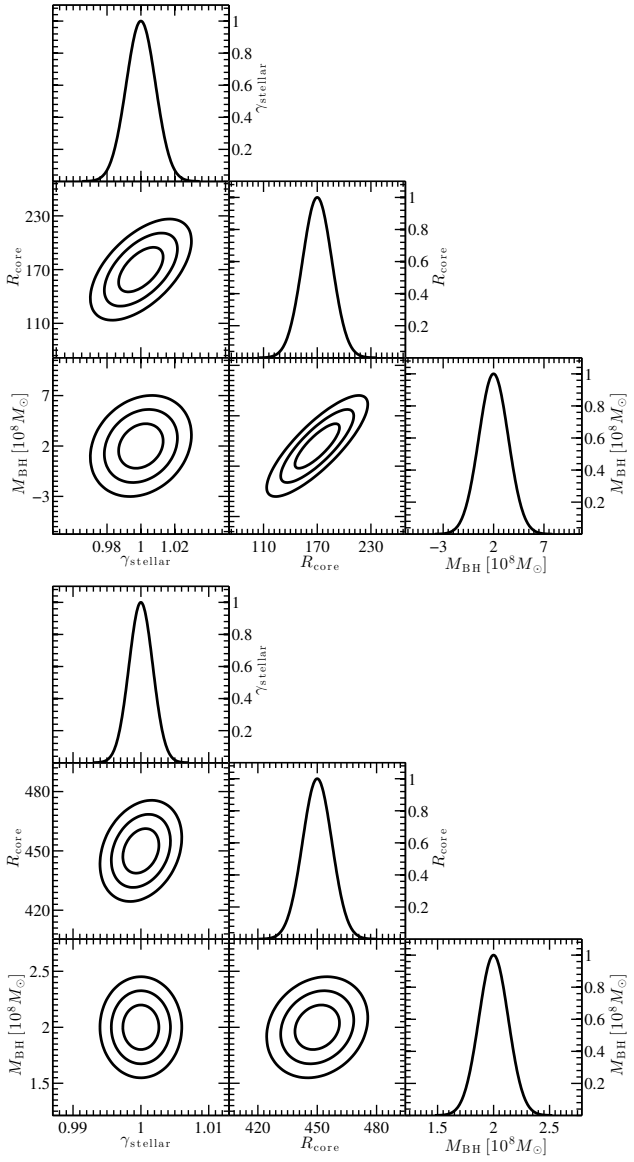

FIG. 4.— Parameter covariance matrices for two simulations (after marginalization over nuisance parameters). Top panel shows that when the core size is small the mass of the SMBH is not measured and only an upper limit can be placed on it. The bottom panel, shows that for larger core sizes, the mass of the SMBH could be measured by high significance.

more massive SMBH. This degeneracy, however, breaks when the core size is very large. Large cores produce more extended central images that are spatially resolved. The distortion caused by a SMBH can distort this image on smaller scales, resulting in a distinct dip in its surface brightness. We found that for cores with a radius larger than 200 pc, central SMBH masses could be measured with high significance (e.g., bottom panel of Figure 4), but for smaller core sizes, only upper limits on the mass of SMBHs can be placed. We also find that when the core size is larger, the constraints on the density profile slope are stronger.

3.3. *Detection of Binary SMBHs*

We also investigated the possibility of detecting binary SMBHs using the perturbations that they induce on lensed central images. We randomly placed two SMBHs with masses of $4 \times 10^8 M_\odot$ each in a circle of radius of 1 kpc from the center of the galaxy and, using the Fisher analysis, computed the detection significance of their masses. We found that in most cases, it is not possible to measure the mass of both SMBHs, either because they are not near the central images

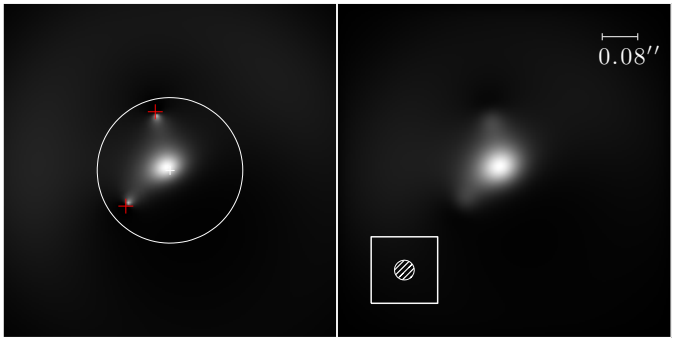

FIG. 5.— Lensing of a central image by two SMBHs with masses of $4 \times 10^8 M_\odot$. The left panel shows the simulated central image. The red crosses show the positions of the SMBHs. The white circle has a radius of 1 kpc from the center of the galaxy. The right panel shows the same data after convolution with the ALMA beam. The beam is shown in the lower panel.

or due to the degeneracy between their masses, their positions, and the core radius, or because the distortions in the central images are unresolved. However, when the central images are fairly extended (due to a shallow density slope and a large core size), a larger fraction of the inner 1 kpc region is covered by the central image, increasing the probability of lensing by SMBHs. Such images also have larger fluxes, increasing the snr of the observations and they also allow for the detection of fairly separated SMBHs. In this case the SMBHs can affect different parts of the central image, reducing the degeneracy between their masses. Under such conditions, we found some configurations that allowed a detection of both SMBH masses. The constraints on SMBH masses in such observations arise from the distortions in the resolved *shape* of the central images. Figure 5 shows an example of such configuration when $\gamma = 0.9$ and $R_{\rm core} = 300$ pc. Left panel shows the central image without the effects of SMBHs and the right panel shows its morphology in presence of two SMBHs.

To estimate the probability of configurations which allow detection of binary SMBHs, we simulated many realizations of the positions of the SMBHs for a high resolution (50 mas) 50-h long observation. We found that $\sim 10\%$ of the simulations, in which the core size was larger than 200 pc, both SMBHs were detected. This number is much larger than what is calculated in Li et al. (2012), since they estimated the probabilities for point sources, appropriate for lensed quasar samples. The extended structure of the background source can significantly increase the probability of

Although this number may seems promising, the prospects of such measurements will be limited by the number of discovered bright central images, which based on their current dearth, may be few. We conclude that, only under rare conditions, and with very long observations (> 40 hours), central image may allow us to probe binary SMBHs. The prospects of such measurement will ultimately depend on discoveries of much larger samples of lenses.

4. CONCLUSION

We have examined the prospects of detecting central, demagnified images of strongly lensed molecular lines with ALMA. We found that there is a non-negligible space of realistic and plausible parameters that result in a high significance detection of the central images. We showed that such deep observations can either allow a measurement of the mass of the central SMBH and the stellar core size, or place strong limits on them. We also studied the possibility of detecting binary SMBHs and found that only under very rare conditions central images may allow detection of both SMBHs.

Acknowledge NSF?

REFERENCES

Barnes, J. E., & Hernquist, L. 1992, ARA&A, 30, 705
Begelman, M. C., Blandford, R. D., & Rees, M. J. 1980, Nature, 287, 307
Bussmann, R. S., Pérez-Fournon, I., Amber, S., et al. 2013, ApJ, 779, 25, 1309.0836
Ebisuzaki, T., Makino, J., & Okumura, S. K. 1991, Nature, 354, 212
Evans, N. W., & Hunter, C. 2002, ApJ, 575, 68, astro-ph/0204206
Ferrarese, L., & Merritt, D. 2000, ApJ, 539, L9, astro-ph/0006053
Ferrarese, L., Côté, P., Jordán, A., et al. 2006, ApJS, 164, 334, astro-ph/0602297
Gebhardt, K., Bender, R., Bower, G., et al. 2000, ApJ, 539, L13, astro-ph/0006289
Golse, G., & Kneib, J.-P. 2002, A&A, 390, 821, astro-ph/0112138
Hezaveh, Y., Dalal, N., Holder, G., Kisner, T., & Kuhlen, M. 2014, ArXiv e-prints, 1403.2720
Hezaveh, Y. D. 2014, ApJ, 791, L41, 1408.3631
Hezaveh, Y. D., & Holder, G. P. 2011, ApJ, 734, 52, 1010.0998
Hezaveh, Y. D., Marrone, D. P., Fassnacht, C. D., et al. 2013, ApJ, 767, 132, 1303.2722
Inada, N., Oguri, M., Keeton, C. R., et al. 2005, PASJ, 57, L7, astro-ph/0503310
Keeton, C. R. 2003, ApJ, 582, 17, astro-ph/0206243
Kormendy, J., & Bender, R. 2009, ApJ, 691, L142, 0901.3778
Kormendy, J., & Ho, L. C. 2013, ARA&A, 51, 511, 1304.7762
Kormendy, J., & Richstone, D. 1995, ARA&A, 33, 581
Li, N., Mao, S., Gao, L., Loeb, A., & di Stefano, R. 2012, MNRAS, 419, 2424, 1110.0887
Negrello, M., Hopwood, R., De Zotti, G., et al. 2010, Science, 330, 800, 1011.1255
Rocha, M., Peter, A. H. G., Bullock, J. S., et al. 2013, MNRAS, 430, 81, 1208.3025
Thomas, J., Saglia, R. P., Bender, R., Erwin, P., & Fabricius, M. 2014, ApJ, 782, 39, 1311.3783
Tremaine, S., Gebhardt, K., Bender, R., et al. 2002, ApJ, 574, 740, astro-ph/0203468
Vieira, J. D., Crawford, T. M., Switzer, E. R., et al. 2010, ApJ, 719, 763, 0912.2338
Vieira, J. D., Marrone, D. P., Chapman, S. C., et al. 2013, Nature, 495, 344, 1303.2723
Wallington, S., & Narayan, R. 1993, ApJ, 403, 517
Weiß, A., De Breuck, C., Marrone, D. P., et al. 2013, ApJ, 767, 88, 1303.2726
Winn, J. N., Rusin, D., & Kochanek, C. S. 2004, Nature, 427, 613, astro-ph/0312136